2013 European Control Conference (ECC)
July 17-19, 2013, Zürich, Switzerland.

# Basal ganglia oscillations: the role of delays and external excitatory nuclei

Ihab Haidar, William Pasillas-Lépine[1], Elena Panteley and Antoine Chaillet

*Abstract*— **Basal ganglia are interconnected deep brain structures involved in movement generation. Their beta-band oscillations (13-30Hz) are known to be linked to Parkinson's disease motor symptoms. In this paper, we provide conditions under which these oscillations may occur, by explicitly considering the role of the pedunculopontine nucleus (PPN). We analyze the existence of equilibria in the associated firing-rate dynamics and study their stability by relying on a delayed MIMO frequency analysis. These results are illustrated with simulations that confirm numerically the analytic predictions of our two main theorems.**

## I. Introduction

Basal ganglia are deep brain structures involved in voluntary motor control as well as cognitive and motivational processes [16]. They have been studied extensively in connection with a variety of pathological observations such as Parkinson's disease [21]. Some evidence suggests that the advance of parkinsonism is highly correlated to the presence of abnormal oscillations in the beta band (13-30 Hz) within the basal ganglia [1]. There exist several hypotheses about the origin of these oscillations. Some of them emphasize the cortical [22] or striatal [13] origin of the phenomenon. But another popular assumption is that these oscillations may originate from the system composed of two excitatory-inhibitory basal ganglia nuclei: the subthalamic nucleus (STN), which is an excitatory nucleus, and the globus pallidus pars externa (GPe), which is an inhibitory nucleus [19]. Since basal ganglia are highly interconnected with the pedunculopontine nucleus (PPN) [7], [12], [14], this nucleus might have an influence on their oscillatory activity. The aim of our paper is to quantify this influence, with the help of control theory tools.

To explore the origin of pathological oscillations in the basal ganglia, some works [20], [8] exploit a microscopic approach in which every neuronal cell is modeled individually. Other works rely on firing-rate models [15], [10], [17], [18]. These models are formulated in terms of an ordinary differential equation that rules the evolution of the number of spikes per time-unit within the considered neuronal population [3]. In [15], the authors exploit a firing-rate model of the STN and GPe populations to derive analytical conditions under which beta oscillations occur. These conditions have been improved in [17], [18] to provide tighter conditions for the existence of oscillations. The particular role of PPN within the basal ganglia has been specifically addressed in [11], where the authors study how the PPN responds to physiological and pathological inputs of the basal ganglia.

Here we develop a mathematical model that describes the interaction between three neuronal populations: PPN, STN and GPe (see Section II). To analyze this model, we extend the approach developed in [17] for two nuclei only. We first study the existence and uniqueness of equilibrium points. We derive necessary and sufficient conditions for the existence of multiple equilibria. Additionally, we propose a sufficient condition for global asymptotic stability in the absence of delays (see Section III). Then, the system is linearized and the MIMO Nyquist stability criterion [2] is applied to the feedback loop of the linearized system. We derive conditions on the delays and interconnection gains for the asymptotic stability of the network, and hence the absence of pathological oscillations (see Section IV). These results are illustrated by numerical simulations (see Section V). The proofs can be found in the preprint version of our paper [4].

## II. Model description

As we mentionned in the introduction, our objective is to analyze pathological oscillations in the basal ganglia. To characterize the firing rate of neural populations in STN, GPe and PPN, we use the well described firing-rate model. The architecture of our model is shown in Figure 1. The STN neurons project excitatory axons to the GPe [16], while GPe neurons project inhibitory axons to the STN and to other GPe neurons [9]. The STN neurons project also excitatory axons to the PPN, which projects back excitatory axons to the STN [14]. Additionally, the

*This work was financially supported by the European Commission through the FP7 NoE HYCON2.

[1]Corresponding author.

Ihab Haidar is with L2S-Supélec, 3, rue Joliot-Curie, 91192, Gif-sur-Yvette, France, ihab.haidar@lss.supelec.fr

William Pasillas-Lépine is with CNRS-L2S-Supélec, same address, pasillas@lss.supelec.fr

Elena Panteley is with CNRS-L2S-Supélec, same address, panteley@lss.supelec.fr

Antoine Chaillet is with Univ. Paris-Sud 11-L2S-Supélec, same address, antoine.chaillet@lss.supelec.fr

STN and PPN nuclei receive inputs from cortex [12], [9], [14] and the GPe nucleus receives input from the striatum [9].

Like in similar models [15], [17], [18], the firing rates of the STN, GPe, and PPN populations, respectively, are ruled by the delayed differential equations

$$\begin{aligned}\tau_s\dot{x}_s &= S_s\big(c_s^p x_p(t-\delta_s^p) - c_s^g x_g(t-\delta_s^g) + u_s\big) - x_s\\ \tau_g\dot{x}_g &= S_g\big(c_g^s x_s(t-\delta_g^s) - c_g^g x_g(t-\delta_g^g) + u_g\big) - x_g\\ \tau_p\dot{x}_p &= S_p\big(c_p^s x_s(t-\delta_p^s) + u_p\big) - x_p\end{aligned} \tag{1}$$

where $x_s$, $x_g$, and $x_p$ represent the firing rates of the STN, GPe and PPN neurons, respectively. By abuse of notation, we omit the dependency of $\dot{x}_i$ and $x_i$ on $t$, for $i \in \{s, g, p\}$. The positive gains $c_s^p$, $c_p^s$, $c_s^g$, $c_g^s$ and $c_g^g$ define the weight of the different synaptic interconnections between these three neuron populations. The variables $u_s$, $u_g$ and $u_p$ describe the external inputs, from the striatum and cortex, received by these populations. The time constants $\tau_s, \tau_g$ and $\tau_p$ describe how rapidly the three populations react to the inputs. We assume that all the delays $\delta_s^p$, $\delta_p^s$, $\delta_s^g$, $\delta_g^s$ and $\delta_g^g$ are nonnegative and constant. The scalar functions $S_s, S_g$ and $S_p$ define the activation functions of STN, GPe and PPN respectively.

*Assumption 1:* For each $i \in \{s, g, p\}$, the activation function $S_i : \mathbb{R} \to (0; 1)$ is continuously differentiable and strictly increasing. Its infimum is equal to 0 and its supremum is equal to 1. In addition, its derivative $S_i'$ is upper-bounded and there exists at least one point at which it reaches its maximum denoted $\sigma_i$.

## III. Analysis in the absence of delays

### A. Existence and uniqueness of equilibrium points

The system (1) is defined everywhere on $\mathbb{R}^3$, since the activation functions are defined on $\mathbb{R}$. Nevertheless, one can check that the unit cube is invariant for this system.

*Lemma 1:* Under Assumption 1, for any constant inputs $u_s, u_g$ and $u_p$, the unit cube

$$D := \{(x_s, x_g, x_p) \in \mathbb{R}^3 : x_s, x_g, x_p \in [0, 1]\}.$$

is positively invariant for the delayed system (1).

The following result analyzes the existence and multiplicity of equilibria of the dynamics (1).

*Theorem 1:* Under Assumption 1, we have that if

$$\sigma_p\sigma_s c_s^p c_p^s \leq 1 \tag{2}$$

then the system (1) has a unique equilibrium point, for each constant vector $(u_s^\star, u_g^\star, u_p^\star) \in \mathbb{R}^3$. Otherwise, there exists a constant vector $(u_s^\star, u_g^\star, u_p^\star)$ for which the system (1) has at least three distinct equilibria. Moreover, if

$$\left(\sigma_p c_s^p c_p^s - \frac{1}{\sigma_s}\right)\left(c_g^g + \frac{1}{\sigma_g}\right) > c_s^g c_g^s \tag{3}$$

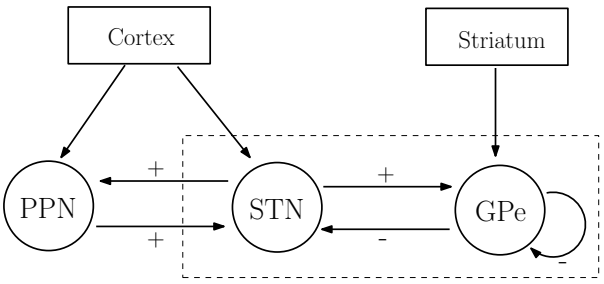


Fig. 1. Schematic diagram of three neuclei: STN, GPe and PPN.

then, for each constant input $u_g^\star$ , there exists a pair of constant input $(u_s^\star, u_p^\star)$ for which the system (1) has at least three distinct equilibria.

Theorem 1 generalizes the equilibrium study given by [17, Theorem 1]. It shows, in particular, that under condition (3), the existence of multiple equilibria can occur even for arbitrarily small striatal input. The proof of Theorem 1 follows the same lines as in [17, Theorem 1] and can be found in [4].

### B. Stability of equilibria

Consider an equilibrium point $x^\star$, associated to a vector of inputs $u^\star$, whose existence is ensured by Theorem 1. Let

$$e = x - x^\star \quad \text{and} \quad v = u - u^\star. \tag{4}$$

The linearization of the dynamics (1) around $x^\star$ is given by

$$\begin{aligned}\tau_s\dot{e}_s &= \sigma_s^\star\big(c_s^p e_p(t-\delta_s^p) - c_s^g e_g(t-\delta_s^g) + v_s\big) - e_s\\ \tau_g\dot{e}_g &= \sigma_g^\star\big(c_g^s e_s(t-\delta_g^s) - c_g^g e_g(t-\delta_g^g) + v_g\big) - e_g\\ \tau_p\dot{e}_p &= \sigma_p^\star\big(c_p^s e_s(t-\delta_p^s) + v_p\big) - e_p\ ,\end{aligned} \tag{5}$$

where

$$\begin{aligned}\sigma_s^\star &:= S_s'(c_s^p x_p^\star - c_s^g x_g^\star + u_s^\star)\\ \sigma_g^\star &:= S_g'(c_g^s x_s^\star - c_g^g x_g^\star + u_g^\star)\\ \sigma_p^\star &:= S_p'(c_p^s x_s^\star + u_p^\star).\end{aligned} \tag{6}$$

We next rely on this linearization to study the stability properties of $x^\star$. We start by considering system (1) in the absence of delays.

*Proposition 1:* Consider the delayed system (1), and assume that

$$\delta_i^j = 0 \quad \text{for} \quad i, j \in \{s, g, p\}. \tag{7}$$

Fix any input vector $u^\star := (u_s^\star, u_g^\star, u_p^\star)^T \in \mathbb{R}^3$, consider an equilibrium $x^\star := (x_s^\star, x_g^\star, x_p^\star)^T$ associated to these input, and let $\sigma_i^\star, i \in \{s, g, p\}$ be defined by (6). Then, under Assumption 1, the following holds.

- If the conditions

$$\left(\sigma_p^\star c_s^p c_p^s - \frac{1}{\sigma_s^\star}\right)\left(c_g^g + \frac{1}{\sigma_g^\star}\right) < c_s^g c_g^s \tag{8}$$

$$\frac{\sigma_s^\star}{\tau_s+\tau_p}\left(\sigma_p^\star c_s^p c_p^s - \frac{1}{\sigma_s^\star}\right) < \frac{\sigma_g^\star}{\tau_g}\left(c_g^g + \frac{1}{\sigma_g^\star}\right) \tag{9}$$

  are both satisfied, then the equilibrium point $x^\star$ is locally exponentially stable.
- If the conditions

$$\sigma_p \sigma_s c_s^p c_p^s < 1 \tag{10}$$

$$\sigma_s(c_s^p + c_s^g) + \sigma_g c_g^s + \sigma_p c_p^s < 2 \tag{11}$$

  are both satisfied then $x^\star$ is globally asymptotically stable.

Section IV is devoted to the study of the preservation of these stability properties in the presence of delays.

## IV. Robustness to delays

In this section, we study the stability properties of the equilibria of (1) by relying on its linearization around an equilibrium point. This system can be described in the frequency domain using the closed-loop transfer functions

$$\begin{aligned} H_s(s) &= \frac{\sigma_s^\star}{\tau_s s+1}\ , \quad H_p(s) = \frac{\sigma_p^\star}{\tau_p s+1} \\ H_g(s) &= \frac{\sigma_g^\star}{\tau_g s + 1 + \sigma_g^\star c_g^g e^{-\delta_g^g s}}, \end{aligned} \tag{12}$$

by the following feedback system $(G, K)$

$$\begin{cases} E = GE' + GV \\ E' = KE \end{cases} \tag{13}$$

where $E = (E_s, E_g, E_p)^T$, and $V = (V_s, V_g, V_p)^T$ are the Laplace transform of $e$ and $v$ (introduced in (4)), and the two transfer matrices $G$ and $K$ are given by the following

$$G(s) = \begin{pmatrix} H_s(s) & 0 & 0 \\ 0 & H_g(s) & 0 \\ 0 & 0 & H_p(s) \end{pmatrix}, \tag{14}$$

$$K(s) = \begin{pmatrix} 0 & -c_s^g e^{-\delta_s^g s} & c_s^p e^{-\delta_s^p s} \\ c_g^s e^{-\delta_g^s s} & 0 & 0 \\ c_p^s e^{-\delta_p^s s} & 0 & 0 \end{pmatrix}. \tag{15}$$

In order to study the stability properties of this linearized system, we make use of the Nyquist Theorem [2, Theorem 9.1.8] for MIMO delayed systems. We stress that here the Nyquist Theorem is applied in its general form in the Callier-Desoer class of scalar irrational transfer functions $\hat{\mathcal{B}}$ (see [2, Definitions 7.1.4 and 7.1.6] for detailed definitions, see also [4, Appendix]). We start by checking the stability of the transfer matrices $G$ and $K$. Noticing that $G$ and $K$ are irrational transfer matrices, we begin by verifying that each of its components belongs to $\hat{\mathcal{B}}$. This is stating by the following result, whose proof is provided in [4].

*Proposition 2:* The entries of the transfer matrices $G$ and $K$ defined in (14)-(15) all belong to the Callier-Desoer class of scalar irrational transfer functions $\hat{\mathcal{B}}$.

The transfer matrix $G$ is not necessarily stable. This comes from the fact that the transfer function $H_g$ is not necessarily stable. However, one can observe that $H_g$ is always stable when $\delta_g^g = 0$. [17, Lemma 3] establishes the existence of a delay margin $\Delta(H_g)$ of $H_g$ such that the transfer function $H_g$ is input-output stable if and only if $\delta_g^g < \Delta(H_g)$. We recall that, for a $\bar{\tau} > 0$, the delay margin of an input-output stable SISO transmittance $H \in \hat{\mathcal{B}}$, is defined by

$$\begin{aligned} \Delta(H) := \sup\{\bar{\tau} > 0 :\ &\text{the feedback } (H, e^{-\tau s}) \\ &\text{is input-output stable } \forall \tau \in [0, \bar{\tau})\}. \end{aligned}$$

A formal definition of input-output stability is given in [2, Definition 9.1.1], see also [4, Definition 1]. To compute the delay margin of $H$ one can associate, at a given frequency $\omega$, its gain $\gamma_H(\omega)$ and phase $\varphi_H(\omega)$ which are defined by the relations

$$\begin{aligned} \gamma_H(\omega) &= 20\log_{10}|H(i\omega)| \\ \varphi_H(\omega) &= \arg\left(H(i\omega)\right. \end{aligned} \tag{16}$$

In our approach, the case where the function $\gamma_H$ is strictly decreasing is of a particular interest. Indeed, in this case, to any strictly proper transfer function $H$ such that $\gamma_H(0) > 0$ we can associate its (gain) crossover frequency $\omega_H$, which is defined as the only frequency such that

$$\gamma_H(\omega_H) = 0. \tag{17}$$

This frequency can be used to define the delay margin $\Delta(H)$ by the relation

$$\Delta(H) = \frac{\pi - \varphi_H\left(\omega_H\right)}{\omega_H}. \tag{18}$$

If $\gamma_H$ is strictly decreasing but $\gamma_H(0) \leq 0$, if $H$ is minimum phase (it has neither unstable poles nor unstable zeroes), then we can still define $\Delta(H) = +\infty$.

Now that the stability properties of $G$ and $K$ are fully known in open loop, we analyze the stability of the feedback system (13). The following result provides a necessary and sufficient condition for the stability of the feedback system (13). Its statement relies on the

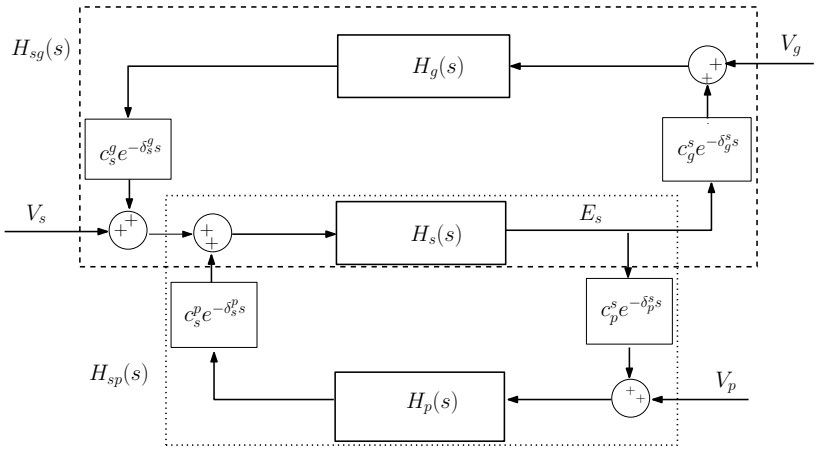


Fig. 2. Bloc diagram of the linearized system (5).

following two transfer functions

$$\begin{aligned} K_p(s) &:= c_p H_p(s) e^{-\delta_p s} \\ K_g(s) &:= -c_g H_g(s) e^{-\delta_g s} \end{aligned} \tag{19}$$

where the quantities

$$\begin{aligned} c_p &:= c_s^p c_p^s \,, & c_g &:= c_s^g c_g^s, \\ \delta_p &:= \delta_p^s + \delta_s^p \,, & \delta_g &:= \delta_g^s + \delta_s^g \end{aligned} \tag{20}$$

are defined in order to obtain a lighter notation.

*Proposition 3:* Suppose that $H_g$ is input-output stable. The feedback system defined by (13) is input-output stable if and only if

$$\text{ind}(1 - H_s(K_p + K_g)) = 0, \tag{21}$$

where $\text{ind}(1 - H_s(K_p + K_g))$ denote the Nyquist index [2, Definition A.1.15] of $1 - H_s(K_p + K_g)$.

The proof of this result is based on standard arguments of the closed-loop stability of delayed MIMO system [2]. It is provided in details in [4]. The remaining aims at giving some insights on how condition (21) can be checked in practice. For this, we represent the feedback system (13) by the block diagram illustrated in Figure 2. This block diagram is composed of two closed-loops, one with external input $(V_s, V_g)$ and the other with external input $(V_s, V_p)$. We introduce the two following transfer functions

$$H_{sp} := \frac{H_s}{1 - H_s K_p} \quad \text{and} \quad H_{sg} := \frac{H_s}{1 - H_s K_g} \tag{22}$$

where $H_{sp}$ and $H_{sg}$ replace the closed-loop marked in dotted and dashed rectangle respectively and which are calculated between $V_s$ and $E_s$.

*Lemma 2:* Suppose that $H_g$ and the feedback systems $(H_s, K_p)$ and $(H_s, K_g)$ are all input-output stable. Then

$$\begin{aligned} \text{ind}\big(1 - H_s(K_p + K_g)\big) &= \text{ind}(1 - H_{sg} K_p) \\ &= \text{ind}(1 - H_{sp} K_g). \end{aligned}$$

According to Lemma 2, if the transfer function $H_g$ and the feedback systems $(H_s, K_p)$ and $(H_s, K_g)$ are input-output stable, then the stability analysis of the feedback system (13) can be equivalently achieved by studying one of the two feedback systems $(H_{sp}, K_g)$ or $(H_{sg}, K_p)$. In what follows, we choose to focus on the feedback system $(H_{sp}, K_g)$ to study the stability of the network of Figure 2. This choice is motivated by the following lemma, which provides conditions under which the gain $\gamma_{H_{sp}}$ is monotonically decreasing, thus considerably simplifying the Nyquist plot analysis.

*Lemma 3:* Consider the transfer function $H_{sp}$ defined by (22). For each positive $\delta_p$ as defined in (20), there exists a positive gain $c_p^\star(\delta_p) > 0$ such that the loop gain $\gamma_{H_{sp}}$ is strictly decreasing for every $c_p = c_s^p c_p^s \in (0, c_p^\star(\delta_p))$.

In order to prove the stability of $H_{sp}$, we can directly invoke [17, Theorem 2]. While the stability of $H_{sp}$ does not depend on the loop delay $\delta_p$, this is not the case for $H_{sg}$. In particular, when $c_g \sigma_g^\star \sigma_s^\star > 1 + c_g^g \sigma_g^\star$, only a finite upper bound on the delay $\delta_g$ can be tolerated. These two observations are formalized by the following statement, proved in [4].

*Lemma 4:* Consider the transfer functions $H_{sp}$ and $H_{sg}$, defined in (22), and let

$$G_{sp} := c_p H_s H_p \quad \text{and} \quad G_{sg} := -c_g H_s H_g, \tag{23}$$

where $H_s, H_g$ and $H_p$ are defined in (12). Consider the constants $\sigma_i^\star$, $i \in \{s, p, g\}$, defined by (6). Then following facts hold:

1) The transfer function $H_{sp}$ is input-output stable if and only if $\delta_p < \Delta(G_{sp})$. If $c_p\sigma_p^\star\sigma_s^\star < 1$ then $\Delta(G_{sp}) = +\infty$, otherwise $\Delta(G_{sp}) \leq 0$.
2) Suppose that $H_g$ is input-output stable. Assuming that the gain $\gamma_{H_{sg}}$ is strictly decreasing, the transfer function $H_{sg}$ is input-output stable if and only if $\delta_g < \Delta(G_{sg})$. If the inequality $c_g\sigma_g^\star\sigma_s^\star < 1 + c_g^g\sigma_g^\star$ then $\Delta(G_{sg}) = +\infty$, otherwise $\Delta(G_{sg}) \in (0, +\infty)$.

With Proposition 3 and Lemmas 2 and 4 at hand, we are now ready to state the following result, which provides conditions for the local exponential stability of the linear system (5).

*Theorem 2:* Consider the delayed differential equation defined by (5). Let $u^\star \in \mathbb{R}^3$ be any input such that, for the equilibrium $x^\star$ associated to these inputs, the transfer functions $H_g, H_{sp}$ and $H_{sg}$, defined in (12) and (22), are input-output stable. Define $H = c_g H_g H_{sp}$. Assume that the gain of $\gamma_H$ is strictly decreasing (which can be verified using Lemma 3 and [17, Lemma 4] together). For every $\delta_p > 0$, $x^\star$ is locally exponentially stable for (5) if and only if $\delta_g < \Delta(H)$.

The previous result gives only conditions for the stability of the linearized system. Nevertheless, in our case, when the linearized system is exponentially stable its hyperbolicity also implies stability properties for the original nonlinear system (1). For more details on this point, we refer the reader to [5, Theorem 4.6] and to [6, Section 10.1].

Using Lemma 3 and the fact that the transfer function $H_g$ can be strictly decreasing [17, Lemma 4], the following result derives directly from Theorem 2.

*Corollary 1:* Consider the delayed differential equation defined by (5). Let $u^\star \in \mathbb{R}^3$ be any input such that, for the equilibrium $x^\star$ associated to these inputs, the transfer functions $H_g, H_{sp}$ and $H_{sg}$ are input-output stable. Assume that the gain of $\gamma_{H_g}$ is strictly decreasing. For each $\delta_p > 0$, there exist $c_p^\star > 0$ such that for each $c_p < c_p^\star$ , $x^\star$ is locally exponentially stable for (5) if and only if $\delta_g < \Delta(H)$.

## V. Numerical simulations

As in [15], the activation functions $S_s, S_g$ and $S_p$ are approximated by a normalized sigmoïd function of the form

$$S_i(x) = \frac{B_i}{B_i + (M_i - B_i)e^{-4x}} \ , \quad i \in \{s, g, p\} \quad (24)$$

where $B_i$ and $M_i$ are given in Table I. These functions satisfy Assumption 1 with $\sigma_i = 1$, for $i \in \{s, g, p\}$.
The parameter values of system (1), and precisely the transmission delays, time-constants, and activations functions, are chosen as follows. For the STN and GPe nuclei, these values are the same as those taken in [15], [17] and they are given in Table I. For the PPN, and since no experimental data is available in the literature, the parameters values are taken equal to those that correspond to the STN.

TABLE I

| Parameter | Value | Description |
|---|---|---|
| $\delta_g^s$ | 6 $ms$ | Delay from STN to GPe |
| $\delta_s^g$ | 6 $ms$ | Delay from GPe to STN |
| $\delta_p^s$ | 6 $ms$ | Delay from STN to PPN |
| $\delta_s^p$ | 6 $ms$ | Delay from PPN to STN |
| $\delta_g^g$ | 4 $ms$ | Internal delay in the GPe |
| $\tau_s$ | 6 $ms$ | STN time constant |
| $\tau_g$ | 14 $ms$ | GPe time constant |
| $\tau_p$ | 6 $ms$ | PPN time constant |
| $M_s$ | 300 $spk/s$ | Maximal firing rate for the STN |
| $B_s$ | 17 $spk/s$ | Firing rate at rest for the STN |
| $M_g$ | 400 $spk/s$ | Maximal firing rate for the GPe |
| $B_g$ | 75 $spk/s$ | Firing rate at rest for the GPe |
| $M_p$ | 300 $spk/s$ | Maximal firing rate for the PPN |
| $B_p$ | 17 $spk/s$ | Firing rate at rest for the PPN |

As in [15], [17] the interconnection gain $c_j^i$ from nucleus $i$ to nucleus $j$ ($i, j \in \{s, g\}$) in the STN-GPe network, is given by

$$c_j^i = {c_j^i}^H + k({c_j^i}^D - {c_j^i}^H) \qquad i, j \in \{s, g\} \qquad (25)$$

where $k$ is a parameter that describes the evolution of Parkinson's disease, ${c_j^i}^H$ and ${c_j^i}^D$ are, respectively, the interconnection gains for the healthy and diseased states (given in Table II). Similarly, the external inputs are given by

$$u_i = {u_i}^H + k({u_i}^D - {u_i}^H) \qquad i \in \{s, g, p\} \qquad (26)$$

where ${u_i}^H$ and ${u_i}^D$ are, respectively, the external inputs for the healthy and diseased state (given in Table II). The external inputs to the PPN, for the healthy and diseased state, are picked equal to that of STN. The parameter $k$ is fixed to $k = 0.2$, value for which the two-dimensional system STN-GPe is locally asymptotically stable [15], [17], [18]. The evolution of system (1) is carried out in function of the interconnection gains $c_p^s$ and $c_s^p$, which are taken equal.

One can easily check the dependency on the parameter $c_p$ (defined in (20)) of the delay margin $\Delta(H)$, by plotting $\Delta(H)$ as a function of $c_p \in (0; 1)$ (see [4]). It can be observed that the delay margin decreases when $c_p$ increases. In addition, one can see that when $c_p = 0.2$ the linear system (5) is approximately at the bifurcation point. After checking the dependency on $c_p$ of $\Delta(H)$, we set two distinct values of $c_p$ around the bifurcation point: $c_p = 0.1$ and $c_p = 0.3$ (note that for these values the gain $\gamma_{H_{sp}}$ is strictly decreasing). We simulate the evolution of nonlinear system (1) together with Nyquist diagram of its linearization (5) in both cases. The results of our simulations are presented in Figure 3A and 3B. When $c_p = 0.1$, we have $\Delta(H) > \delta_g$, the Nyquist plot does not encircle the critical point, and the nonlinear

TABLE II

| Parameter | Healthy state | Diseased state |
|---|---|---|
| $c_g^s$ | 14.3 | 15 |
| $c_s^g$ | 1.5 | 14.3 |
| $c_g^g$ | 6.6 | 12.3 |
| $u_s$ | 0.2 | 0.8 |
| $u_g$ | 0.1 | 0.7 |
| $u_p$ | 0.2 | 0.8 |

system (1) exhibits no oscillations after transients. When $c_p = 0.3$, we have $\Delta(H) < \delta_g$, the critical point is encircled, and the nonlinear system (1) shows sustained oscillations. These oscillations are in the beta band (28 Hz), hence likely to yield pathological symptoms.

## VI. Conclusion

Based on a firing-rate model, we have studied the role of an external excitatory nucleus (PPN) in the generation of pathological oscillations within the basal ganglia. By Theorem 1, we show the capacity of the weight of interconnections between the PPN and the basal ganglia to change the firing-rate steady states of each nucleus. Then, by Theorem 2, we show how the transmission delays can intervene together with the interconnection gains in the modulation of these oscillations. These results are illustrated with numerical simulations.

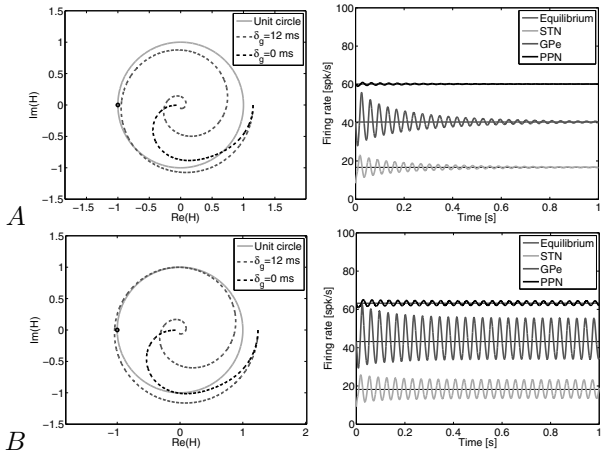


Fig. 3. Influence on stability of the interconnection gain $c_p^s$ and $c_s^p$, for $k = 0.2$. On the left, the open-loop frequency-response is represented in a Nyquist diagram. On the right, the temporal evolution of the system (1) is plotted.

## References


[1] T. Boraud, P. Brown, J.A. Goldberg, A.M. Graybiel, and P.J. Magill. Oscillations in the basal ganglia: the good, the bad, and the unexpected. *Advances in behavioral biology (The Basal Ganglia VIII, Editors: Bolam, J.P., Ingham, C.A. and Magill, P.J.*, 56:1–24, 2005.

[2] R.F. Curtain and H. Zwart. *An introduction to infinite-dimensional linear systems theory*, volume 21. Springer-Verlag, April 1995.

[3] P. Dayan and L.F. Abbott. Computational and mathematical modelling of neural systems. *Theoretical neuroscience, MIT Press*, 2001.

[4] I. Haidar, W. Pasillas-Lépine, E. Panteley, and A. Chaillet. Basal ganglia oscillations: the role of delays and external excitatory nuclei. *Preprint available at, http://hal.archives-ouvertes.fr/hal-00742100/.*

[5] A. Halanay. *Differential equations*, volume 23. Elsevier, 1966.

[6] J.K. Hale and S.M.V. Lunel. *Introduction to functional differential equations*, volume 99. Springer, 1993.

[7] C. Hammond, B. Rouzaire-Dubois, J. Feger, A. Jackson, and A.R. Crossman. Anatomical and electrophysiological studies on the reciprocal projections between the subthalamic nucleus and nucleus tegmenti pedunculopontinus in the rat. *Neuroscience*, 9(1):41–52, 1983.

[8] H.K. Khalil. *Nonlinear systems*. Prentice Hall, 2002.

[9] H. Kita. Globus pallidus external segment. *Prog Brain Res.*, 160:111–133, 2007.

[10] A. Leblois, T. Boraud, W. Meissner, H. Bergman, and D. Hansel. Competition between feedback loops underlies normal and pathological dynamics in the basal ganglia. *The Journal of Neuroscience*, 26(13):3567–3583, March 2006.

[11] M.A.J. Lourens, H.G.E. Meijer, T. Heida, E. Maranib, and S.A. van Gils. The pedunculopontine nucleus as an additional target for deep brain stimulation. *Neural Networks*, 24(6):617–630, 2011.

[12] C. Martinez-Gonzalez, J. Paul-Bolam, and J. Mena-Segovia. Topographical organization of the pedunculopontine nucleus. *Front Neuroanat.*, 5(22), April 2011.

[13] N.M McCarthy, C. Moore-Kochlacs, X. Gu, E.S. Boyden, X. Han, and N. Kopell. Striatal origin of the pathologic beta oscillations in parkinson's disease. *Proc. of the National Academy of Sciences*, 108(28):11620–11625, 2011.

[14] J. Mena-Segovia, J.P. Bolam, and P.J. Magill. Pedunculopontine nucleus and basal ganglia: distant relatives or part of the same family? *Trends in Neurosciences*, 27(10):585–588, October 2004.

[15] A.L. Nevado-Holgado, J.R. Terry, and R. Bogacz. Conditions for the generation of beta oscillations in the subthalamic nucleus-globus pallidus network. *The Journal of Neuroscience*, 30(37):12340–12352, September 2010.

[16] J.A. Obeso and J.L. Lanciego. Past, present, and future of the pathophysiological model of the basal ganglia. *Front Neuroanat.*, 5(39), July 2011.

[17] W. Pasillas-Lépine. Delay-induced oscillations in wilson and cowan's model: An analysis of the subthalamo-pallidal feedback loop in healthy and parkinsonian subjects. *Biological Cybernetics*, Accepted for publication, 2013.

[18] A. Pavlides, S.J. Hogan, and R. Bogacz. Improved conditions for the generation of beta oscillations in the subthalamic nucleus-globus pallidus network. *European Journal of Neuroscience*, 36:2229–2239, 2012.

[19] D. Plenz and S.T. Kital. A basal ganglia pacemaker formed by the subthalamic nucleus and external globus pallidus. *Nature*, 400(6745):677–682, August 1999.

[20] D. Terman, J.E. Rubin, A.C. Yew, and C.J. Wilson. Activity patterns in a model forthe subthalamopallidal network of the basal ganglia. *The Journal of neuroscience*, 22(7):2963–2976, 2002.

[21] J.R. Walters, D. Hu, C.A. Itoga, L.C. Parr-Brownlie, and D.A. Bergstrom. Phase relationships support a role for coordinated activity in the indirect pathway in organizing slow oscillations in basal ganglia output after loss of dopamine. *Neuroscience*, 144(2):762–776, January 2007.

[22] N. Yamawaki, I.M. Stanford, S.D. Hall, and G.L. Woodhall. Pharmacologically induced and stimulus evoked rhythmic neuronal oscillatory activity in the primary motor cortex in vitro. *Neuroscience*, 151(2):386–395, 2008.